LEGIBILITY NOTICE

A major purpose of the Technical Information Center is to provide the broadest dissemination possible of information contained in DOE's Research and Development Reports to business, industry, the academic community, and federal, state and local governments.

Although a small portion of this report is not reproducible, it is being made available to expedite the availability of information on the research discussed herein.

LA-UR-87-3519

/ CVT LA-UR--87-3519

DE88 001791

Los Alamos National Laboratory is operated by the University of California for the United States Department of Energy under contract W-7405-ENG-36

TITLE: Bidirectional Electron Heat Flux Events In Space

AUTHOR(S): S.J. Bame and J.T. Gosling

SUBMITTED TO Chapter in book entitled "Laboratory and Space Plasmas, to be edited by Prof. H. Kikuchi, published by Springer Verlag, NY, 1987-88. (Proceedings of the Tokyo plasm workshop, November 1986).

DISCLAIMER

Los Alamos Los Alamos National Laboratory
Los Alamos, New Mexico 87545

BIDIRECTIONAL ELECTRON HEAT FLUX EVENTS IN SPACE

S. J. Bame and J. T. Gosling
Los Alamos National Laboratory, Los Alamos NM 87545, USA

INTRODUCTION

During the last three decades much progress has been made toward exploring and understanding the plasma environment of our Earth and solar system. Space satellites and probes have outlined the major plasma structures and regimes found surrounding Earth and other solar system bodies as well as those found in interplanetary space near the ecliptic plane. Studies of these plasmas have contributed to a more complete understanding of plasmas in general, including astrophysical and laboratory plasmas. Similarly, studies of laboratory plasmas and plasma theory have contributed to a more profound understanding of the nature of space plasmas, their sources and sinks, processes which contribute to stable plasma regimes on the one hand, and instabilities that disrupt plasma regimes on the other hand.

In this paper we discuss a number of space plasma phenomena which have been illuminated by a powerful diagnostic tool provided by tracing heat flux carried by the solar wind. Measurements of this flow of heat energy from the sun and other hot plasma regions have been employed to increase our understanding of the solar wind interaction with solar system objects. Similarly, anomalies in the heat flux have helped to explain unusual plasma entities which are sometimes found in the interplanetary solar wind. The heat flux is principally carried by the solar wind electrons, since they are much more mobile than the ions. The electrons conduct heat outward from the hot solar corona and in a sense they constitute test particles that trace out the various plasma structures found in the solar wind and in the vicinities of bodies immersed in the interplanetary plasma flow.

In the following sections we begin by discussing the electron heat flux which flows outward from the solar corona. This flux is ordinarily found flowing in one direction, i.e., it is unidirectional. Sometimes it is observed counterstreaming, i.e., it is bidirectional. In later sections we discuss how detection of bidirectional heat fluxes has contributed to a more complete understanding of the Earth's bow shock, the bow wave at Comet Giacobini-Zinner, interplanetary plasma structures injected into the solar wind by solar activity processes, and finally polar rain electrons that are found precipitating over the Earth's poles but are believed to originate in the hot solar corona.

This paper is not intended to be a comprehensive review of all of the work done in this field. We rely principally on Los Alamos experiment results to illustrate the bidirectional heat flux phenomena selected for discussion, but refer to other results as appropriate.

UNIDIRECTIONAL AND BIDIRECTIONAL ELECTRON HEAT FLUXES

It has been known for some years that the electron component of the solar wind plasma carries heat away from the hot solar corona in the form of a heat flux [*Montgomery et al.*, 1968]. As depicted schematically in Figure 1, this outward conduction of heat is a consequence of the fact that the corona, which contains plasma at temperatures above 10^6 K, connects to the much cooler outer reaches of the heliosphere through the interplanetary magnetic field, IMF.

Figure 1 is a highly simplified representation of the inner heliosphere extending from the sun to beyond the Earth's orbit at 1 AU. The figure assumes a solar wind which is flowing radially outward with a uniform 400 km s^{-1} bulk velocity. The flow is shown without high speed streams which emanate from coronal holes (see, for example, the review by *Hundhausen* [1977]) or slower flows which develop from coronal streamers [*Gosling et al.*, 1981]. Although idealized, this uniform Archimedean spiral configuration illustrates the general field topology governing the unidirectional outflow of heat from the hot corona. Electrons with energy above $\sim$ 80 eV escape from the collective bulk plasma flow of electrons and ions near the sun and propagate relatively freely along the IMF. At these higher energies, the electron coulomb scattering lengths are long, comparable to Earth's orbital distance. At lower energies coulomb scattering constrains

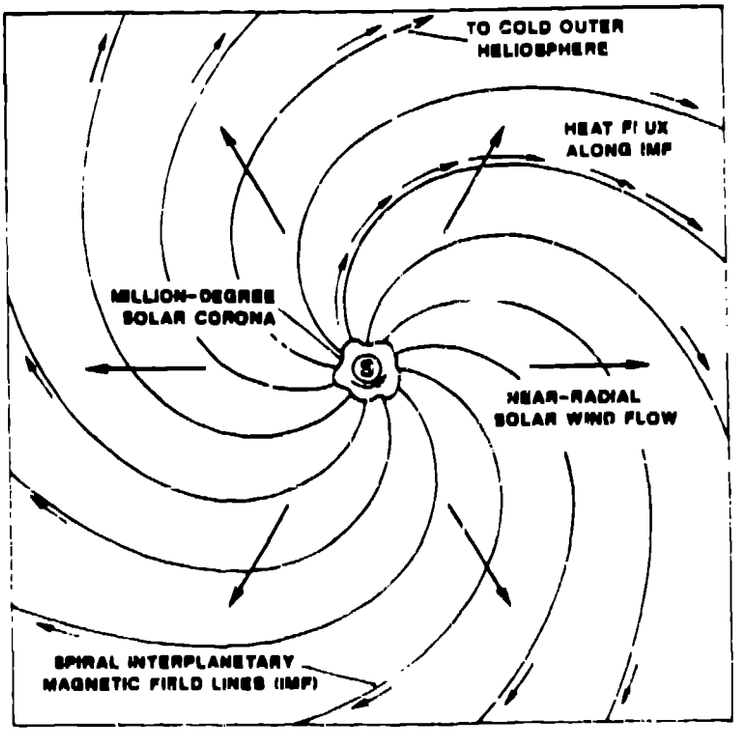

Fig. 1. Schematic representation of an idealized inner heliosphere. Rotation of the sun causes the IMF lines, pulled outward by a constant 400 km s^{-1} radial solar wind flow, to form an Archimedean spiral configuration. Earth's orbit lies at the radius where the spiral angle is $\sim$ 45°. A unidirectional heat flux from the hot corona carried by electrons with energies of $\sim$ 80 eV and higher propagates toward the cold outer heliosphere along the field lines (shown here along one line and at the extremes of the others). In this simplified representation variations in flow speed, which significantly alter the uniform spiral configuration, are neglected.

the electrons so that they remain within the collective plasma flow. The higher energy electrons, in effect, act as test particles tracing out the IMF geometry.

Consequently, as shown in Figure 2(a), solar wind electrons measured in interplanetary space normally display two distinct velocity distribution components [*Montgomery et al.*, 1968]: 1) a cooler component called the "core" which contains the bulk of the electron population, and 2) a more tenuous component of higher temperature electrons, called the "halo." The core tends to be nearly isotropic and can usually be well represented by a bi-Maxwellian distribution function from which the standard bulk properties of the plasma, such as density, speed, and the parallel and perpendicular electron temperature components, can be derived. On the other hand, the halo component is usually less isotropic, is aligned along the IMF in the direction pointing outward from the sun, and is composed of coronal electrons carrying the heat flux from the hot corona toward the cold outer reaches of the heliosphere. Sometimes the heat flux is broad and not well distinguished, while at other times it can be very narrow, particularly in high speed streams. Such a narrow distribution has been termed the "strahl" by *Rosenbauer et al.* [1977], but in this paper we do not distinguish between the broad and narrow halo distributions and include both under the generic term "heat flux."

Under special conditions, to be discussed in the following sections, both ends of the IMF may be connected to hot sources, resulting in a bidirectional heat flux, i.e., heat fluxes flowing in opposite directions or counterstreaming along the IMF, as shown in Figure 2(b). Experience shows that the oppositely directed heat flux distributions need not be symmetric. They can have both unequal widths and unequal flux intensities. In the following sections we give examples of several plasma regimes in which bidirectional heat fluxes are a prominent feature.

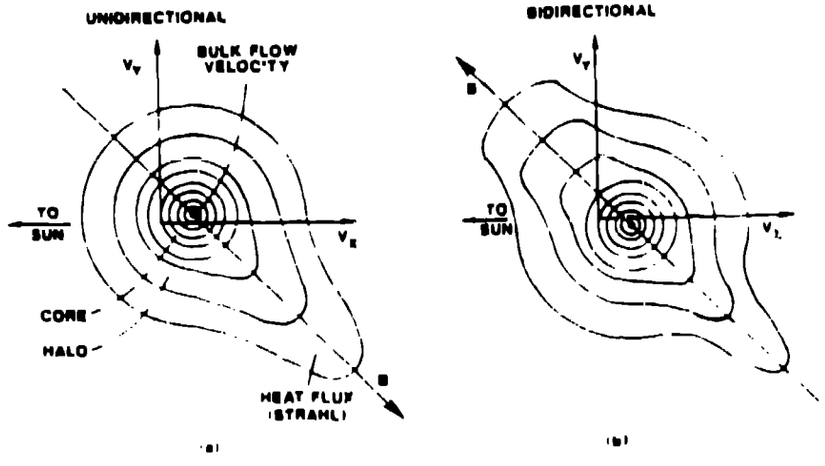

Fig. 2.(a) Schematic solar wind electron velocity distribution shown in an isointensity contour representation. The distribution, as discussed in the text, is composed of an inner core which contains most of the electrons and a tenuous halo of higher energy electrons which carries a unidirectional heat flux from the corona along the IMF. The solar wind bulk flow velocity is represented by the central dot. (b) A bidirectional heat flux distribution oriented along the IMF. The forward and backward heat fluxes can have different intensities and widths.

BIDIRECTIONAL HEAT FLUX AT THE BOW SHOCK

When a spacecraft is located upstream from the Earth on an IMF line which connects to the bow shock, bidirectional heat flux distributions are commonly observed [*Ogilvie et al.*, 1971; *Feldman et al.*, 1973]. In addition to the usual outward directed heat flux from the sun's hot corona, a heat flux conducting upstream from the bow shock is observed. This is shown schematically in Figure 3 for an IMF orientation that includes some examples of field lines connecting to the bow shock and others that do not connect. Upstream from the shock on field lines which connect to it, solar wind electron distributions exhibit an inner core distribution and two heat flux components. One component depicted by the open elliptical section pointed toward the bow shock represents the outward heat flux from the corona while the oppositely directed and filled-in section represents the backstreaming heat flux from the bow shock. Downstream from the shock but outside it on these same field lines both heat flux components are present, but in this case both are directed to the outer heliosphere. On field lines that do not connect, only the outward coronal component is observed.

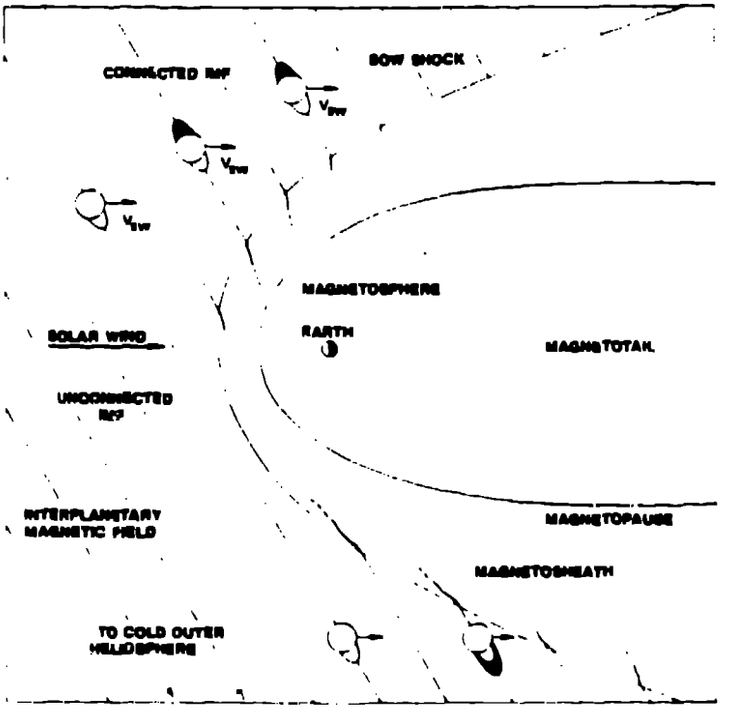

Fig. 3. Schematic representation of the magnetosphere and bow shock immersed in the solar wind. Electron distributions on IMF lines that are connected to the bow shock show a heat flux component from the shock in addition to the usual heat flux from the sun. Field lines are not shown in the magnetosheath since most of them would fall out of the plane of this projection as they drape around or interconnect with the magnetosphere.

The IMF at 1 AU is often quite irregular with fluctuations in both field orientation and field intensity commonly occurring on virtually all time scales. These irregularities are caused by a variety of processes which shall not concern us here; however, because of fluctuations in field orientation, spacecraft connections to the bow shock are usually transitory. Figure 4, which provides a grey scale time history of electron

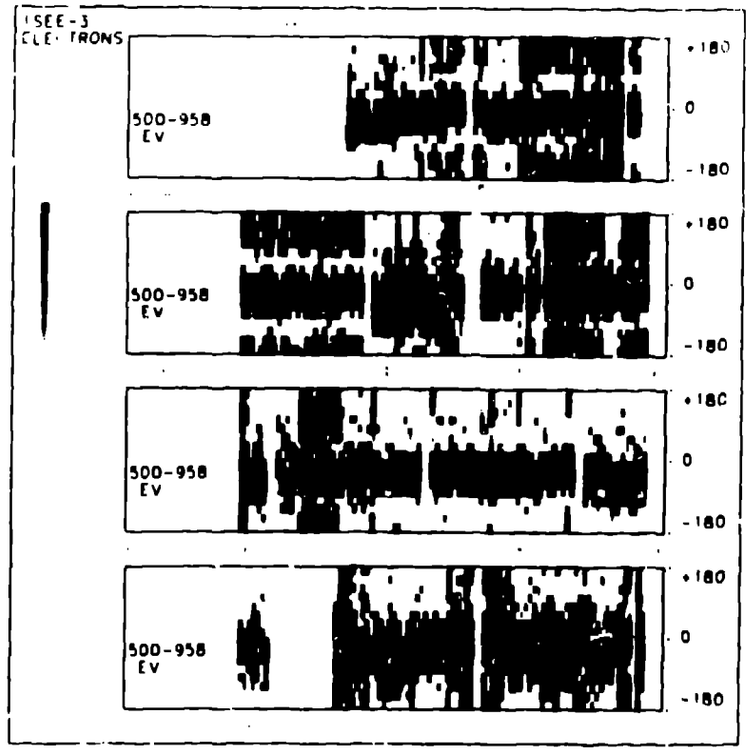

Fig. 4. A gray scale time history representation of ISEE 3 solar wind electron angular distributions with an energy passband extending from 500 to 958 eV measured on Oct. 17, 1982. As indicated by the vertical bar on the left, gray coding of the angular distributions is related to the log of the measured counts within ±67.5° of the spacecraft equatorial plane. Numbers at the right-hand edge of the panels refer to the azimuthal look angle of the measurement, 0° corresponding to the solar direction. The energy passband shown is dominated by the halo population which carries the electron heat flux.

angular distributions in an energy passband from 500 to 958 eV measured upstream from the Earth's bow shock, illustrates the sporadic nature of connections to the shock. Whereas the normal solar wind heat flux is always present in this interval (producing the more or less steady enhancement running across the middle of each panel), the backstreaming fluxes from the bow shock, which produce enhancements near ±180°, are intermittent. Notice that the backstreaming fluxes from the shock in this time interval are also considerably broader in angle than is the heat flux from the sun.

Early measurements of bidirectional heat fluxes associated with the bow shock were made on spacecraft in the upstream solar wind relatively near to the bow shock. These measurements were made by instruments on OGO 5 [*Ogilvie et al.*, 1971], and IMP 6, 7, 8 [*Feldman et al.*, 1973; 1975]. Later measurements made with the Max Planck/Los Alamos fast plasma experiment [*Bame et al.*, 1978a] on ISEE 2 were also obtained near the bow shock [*Feldman et al.*, 1983]. More recent measurements [*Feldman et al.*, 1982] were made far from the Earth with the Los Alamos electron spectrometer on ISEE 3 [*Bame et al.*, 1978b]. A statistical survey of the interplanetary magnetic field orientations that were associated with these bidirectional electron heat fluxes observed with ISEE 3 during the period January 20, 1979 to January 20, 1980 has been completed by *Stansberry et al.*, [1987]. During this period the spacecraft, orbiting the L1 Lagrangian point ~ 220 R_E upstream toward the sun, was sufficiently far from the Earth that it was not usually magnetically

connected to the bow shock. Nevertheless, as noted above, a backstreaming electron heat flux from the shock was observed at ISEE 3 at times.

The observation geometry of the Stansberry *et al.* study is shown in Figure 5(a). ISEE 3, orbiting the L1 point, is positioned at a radius r from the Earth. ψ is the acute angle between the local IMF and the spacecraft position vector relative to the Earth. X_{GSE}, Y_{GSE}, and Z_{GSE} have the conventional geocentric-solar ecliptic definitions. As shown in Figure 5(b), when the IMF was oriented within 5° of the Earth-spacecraft line, backstreaming electrons from the bow shock were clearly observed approximately 18% of the time, perhaps a surprisingly small fraction for this connection geometry. Some connections apparently occurred for angles as large as $\sim 30 - 35°$. The data indicate that a significant portion of the bidirectional events identified with $\psi > 40°$ should be assigned to a category of events other than bow shock connections. Perhaps some of these may be related to the coronal mass ejection events discussed in a later section.

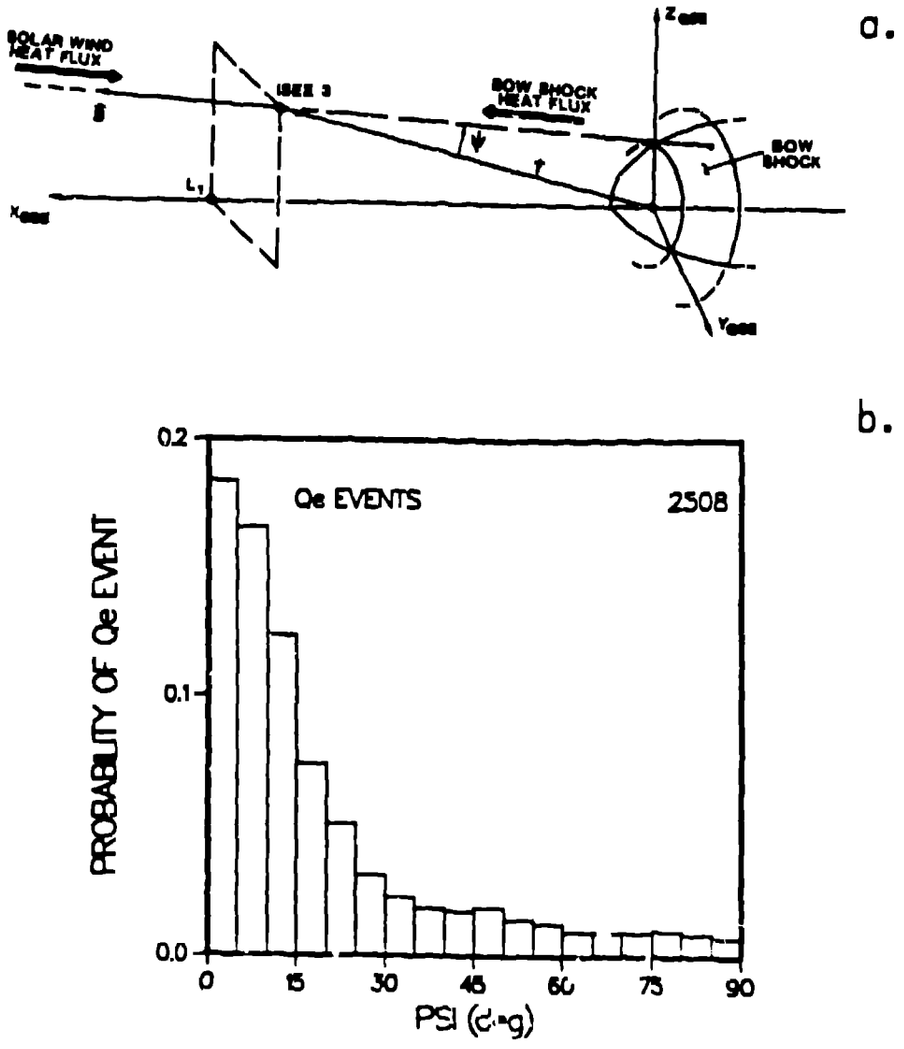

Fig. 5(a) ISEE 3 in orbit around the Sun Earth L1 Lagrangian point in relation to the Earth's bow shock and the interplanetary magnetic field. For a range of cone angles, ψ, the field connects ISEE 3 to the shock, and bidirectional electron heat fluxes can be observed. (b) Histogram showing the probability of observing a bidirectional electron heat flux event for a given cone angle, ψ. Bidirectional heat fluxes known to be of interplanetary origin have been excluded from the data set. Adapted from *Stansberry et al.* [1987]

BIDIRECTIONAL ELECTRON HEAT FLUXES AT COMET GIACOBINI-ZINNER

On September 11, 1985 the International Cometary Explorer (ICE) spacecraft, formerly ISEE 3, passed through the coma and developing tail of Comet Giacobini-Zinner, 7800 km behind the nucleus. The Los Alamos plasma electron experiment on board ICE [*Bame et al.*, 1978b] detected a strong interaction between the solar wind and the comet [*Bame et al.*, 1986]. Highly turbulent, hot, and dense plasma was observed as ICE approached and receded from the central axis of the tail [*Gosling et al.*, 1986a; *Thomsen et al.*, 1986]. In the central tail a narrow, high-density core of very cold plasma was found [*Zwickl et al.*, 1986; *McComas et al.*, 1987] in which the interplanetary magnetic field, draped around the comet, underwent an expected field reversal at a current sheet [*Smith et al.*, 1986; *Slavin et al.*, 1986]. No evidence was found for a conventional, small scale bow shock separating the interaction zone surrounding the comet from the solar wind at the ICE intercept points. Instead, a more gradual transition was observed which has been called a "bow wave" [*Smith et al.*, 1986].

As the spacecraft approached and receded from the region of strong interaction at the comet, episodes of bidirectional electron heat fluxes were observed in the solar wind. These were interpreted in the same way that bidirectional distributions observed in the vicinity of Earth's bow shock have been interpreted except that at the comet it is not clear whether the bow wave is a bow shock modified by the presence of the much heavier cometary ions, or some other kind of a transition. Examples of IMF connected and unconnected electron distributions are shown in Figure 6. Each distribution was measured during a 3-second spin of the spacecraft in which 16 energy sweeps were obtained in 16 azimuthal angle ranges which together cover 360°. The distributions shown in the figure plot log counts vs log energy at the 16 azimuth positions. In the unconnected distribution, measured at 0841:23 UT on September 11, 1985, a clear, unidirectional heat flux is present, flowing outward along the interplanetary magnetic field. Earlier, at 0826:36 UT, the spacecraft was on a field line that connected to the bow wave and hot cometary interaction region. This distribution also displays the central heat flux of hot electrons from the solar corona, but in addition, at

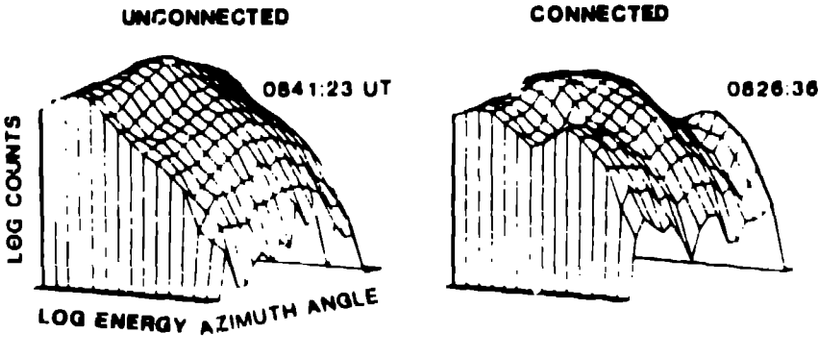

Fig. 6. Examples of connected and unconnected electron counting rate distributions obtained in the upstream region at Comet Giacobini-Zinner. The distributions consist of 16 energy spectra taken at evenly spaced azimuthal angles in one spacecraft spin. From *Bame et al.* [1986].

course, is the heat flux flowing back upstream along the IMF from the hot cometary interaction zone.

A number of bidirectional episodes were detected before ICE entered the bow wave region at ~ 0920 UT [*Bame et al.*, 1986; *Fuselier et al.*, 1986]. Others were observed after the spacecraft had passed through the coma and tail of the comet and had re-entered the solar wind at ~ 1220 UT. Figure 7 shows a plot of electron parameters during an interval of one hour prior to entry into the bow wave at ~ 0920 UT.

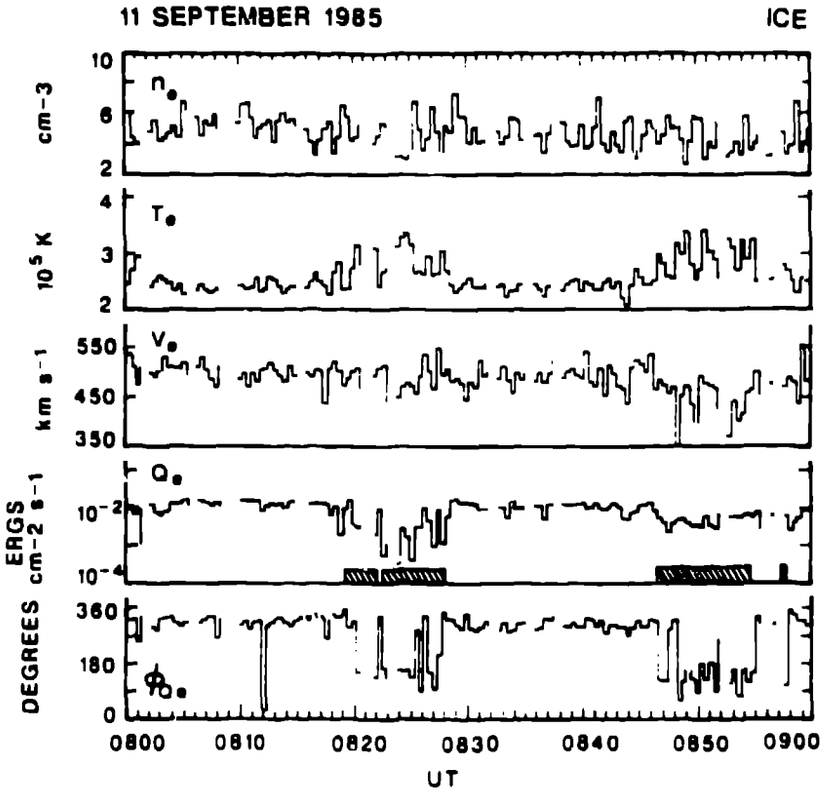

Fig. 7. Electron parameters from a one-hour period measured while ICE was in the upstream solar wind, outside of the bow wave in front of the comet. From *Bame et al.* [1986].

Electron density, n_e, temperature, T_e, and bulk flow speed, V_e, are shown in the top three panels. In the bottom panels, net heat flux, Q_e, and direction of net heat flux, Φ_{Q_e}, are plotted. The cross-hatched bars in the Q_e panel show time intervals when the IMF was connected to the solar wind interaction region surrounding the nucleus of the comet. At these times the temperature is elevated and the net heat flux is reduced, since the coronal heat flux and the cometary heat flux have similar intensities but are oppositely directed. The net heat flux direction switches from an outward flow at ~ 315° to a flow inward toward the sun at ~ 135° during the time intervals highlighted by the bars since the heat flux escaping from the bow wave locally exceeds that coming from the sun.

The single intercept of ICE with the Comet Giacobini-Zinner coma and tail provides only entry and exit points as the cometary bow wave is traversed. It is, of course, desirable to extend our knowledge of the three-dimensional shape of the strong interaction region at the comet. Fortunately, the episodes

and the comet gas production rate [*Fuselier et al.*, 1986]. The backstreaming heat fluxes were observed intermittently in the upstream region as the IMF orientation fluctuated and contact was made and broken with the bow wave. Assuming that the first and last points of contact during an episode of connection occur when $\overline{B}$ is tangent to the bow wave surface, the onsets and ends of upstream heat flux events can be used to infer the location of this boundary. The combination of spacecraft location and magnetic field directions from the vector helium magnetometer carried on ICE [*Smith et al.*, 1986] for all onsets and ends determine a set of field lines tangent to the bow wave boundary. This set was used to find the best fit of an assumed shape, chosen to be a paraboloid of revolution about an axis pointing from the G-Z nucleus toward the sun.

The best fit shape is shown in Figure 8, along with the calculated points derived from the episodes of connection. Some of the scatter in the boundary points is thought to be due to the simplifying assumption that the magnetic field lines from the spacecraft to the points of tangency are straight. Large amplitude MHD-like waves with periods of 1-2 minutes were observed in the upstream region [*Tsurutani* and *Smith*, 1986], so the assumption of straight field lines is somewhat compromised. Inaccuracies caused by this effect were minimized by using one minute averaged magnetic field data.

Assuming that a shock exists at the subsolar standoff point, the calculated subsolar standoff distance of 4×10^4 km was used to estimate a gas production rate of the comet (see *Fuselier et al.* [1986] for details). The computed rate was 3×10^{28} mol/s which is in reasonable accord with estimates from ground-based observations.

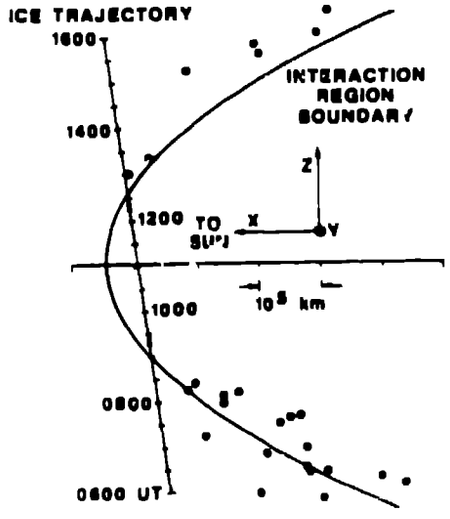

Fig. 8. Location of the cometary bow wave determined from the backstreaming heat flux events. The smooth curve is the best-fit shape of an assumed paraboloid of revolution fitted to the individual points determined from 18 inbound and 7 outbound events. The ICE intercept trajectory projected into the X-Z plane is shown. From *Fuselier et al.* [1986].

On occasion solar wind electrons with energies greater than about 80 eV are observed to be collimated both parallel and antiparallel to the IMF even when a spacecraft clearly is not magnetically connected to the Earth's bow shock. An example of such an interplanetary event can be seen in Figure 9 which displays grey scale-coded electron count rate angular distributions from ISEE 3 in an energy passband extending from 137 to 362 eV as a function of time on Nov. 24 and 25, 1978. The unidirectional beam prior to 2000 UT on November 24 and after ~1700 UT on November 25 is the usual solar wind electron heat flux: changes in the beam azimuth as a function of time correspond to changes in the azimuth of the IMF. (From ~1000 UT until ~1200 UT on November 25 the IMF was tilted strongly out of the ecliptic in such a manner that the IMF and electron heat flux were not centered within the ±67.5° acceptance fan of the ISEE 3 electron analyzer.) Beginning at ~2000 UT on November 24 and continuing until ~0915 UT on November 25 two counterstreaming beams of electrons were observed which constitute a bidirectional electron heat flux event. Note that the counterstreaming beams were of comparable, although not necessarily equal, intensity.

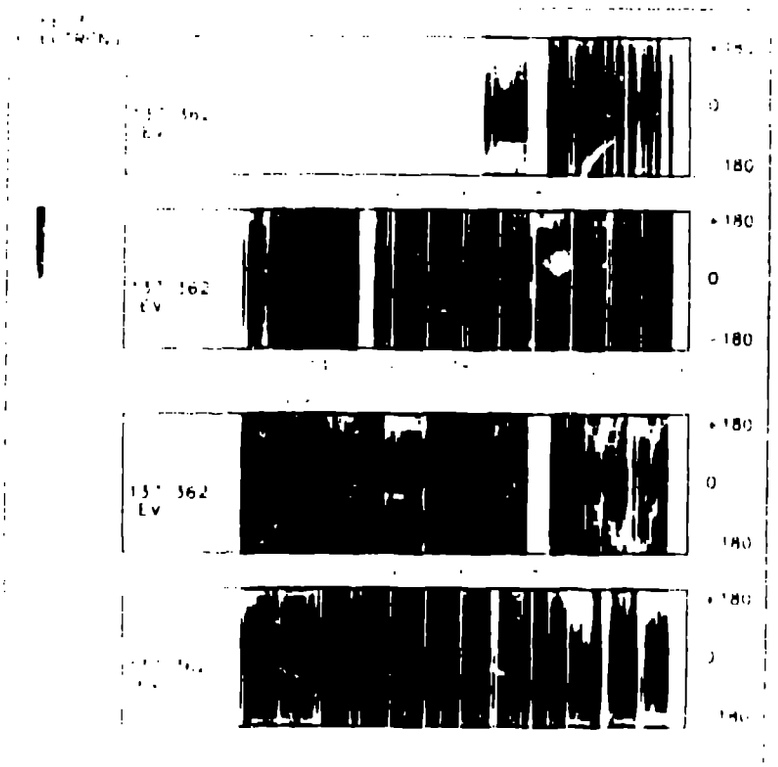

Fig. 9. A grey scale representation of measured solar wind electron angular distributions within an energy passband extending from 137 to 362 eV on November 24–25, 1978. As indicated by the vertical bar on the left, grey scale coding of the angular distributions is related to the log of the number of counts measured within ±67.5° of the spacecraft equatorial plane. Numbers at the right-hand edge of the panels refer to the azimuthal look angle of the measurement, 0° corresponding to the solar direction. The energy passband shown is dominated by the halo population which carries the electron heat flux. Note the onset of an intense bidirectional heat flux event at ~2000 UT on November 24, 1978. Adapted from *Gosling et al.* [1987].

displayed in Figure 9 are observed about 3 times per month [*Gosling et al.*, 1987]. Event durations range from less than one hour to greater than 40 hours; however, the 13-hour duration of the November 24-25 event is representative of the majority and corresponds to a structure with a spatial width or thickness of ~0.13 astronomical units, AU. The onset of electron bidirectionality usually signals spacecraft entry into a distinct plasma and field entity, most often characterized by anomalously low proton and electron temperatures, a strong, smoothly varying magnetic field, a low plasma beta, and a high total pressure. About half of all events exhibit abnormally high helium abundances (He^{++}/H^{+}). Often entry to and/or exit from a bidirectional event is marked by a field rotation discontinuity, and, at times, the field internal to the event rotates through approximately 180° (such a rotation was absent in the November 24-25, 1978 event shown in Figure 9).

The above plasma and field signatures provide information concerning the origin of interplanetary bidirectional heat flux events. However, perhaps the best clue to their origin is their strong association with interplanetary shocks [e.g., *Montgomery et al.*, 1974; *Bame et al.*, 1981; *Zwickl et al.*, 1983; *Gosling et al.*, 1987]; statistical studies reveal that approximately half of all interplanetary bidirectional events are preceded by shocks and that approximately half of all interplanetary shocks are followed within ~24 hours by one or more bidirectional electron heat flux events. Figure 10 illustrates this association for the major shock disturbance of November 12-13, 1978 [*Bame et al.*, 1981]. Shock passage can be distinguished in the vertically stacked ion energy/charge (E/q) spectra on the left-hand side of the figure by the broadening of the spectra and the shift to higher E/q values at ~0028 UT on November 12. Approximately 17 hours later the spacecraft entered a plasma regime characterized by a low ion temperature (narrow spectral peaks), a high helium abundance (large second peak), a moderately strong and steady IMF (not shown), and a strong bidirectional electron heat flux aligned with the IMF (right-hand panel). Importantly, in view of the interpretation to follow, this plasma was flowing faster (peak E/q value higher) than the ambient plasma ahead of the shock. A representative snapshot of contours of the 2-dimensional electron velocity distribution during the interval of intense bidirectional streaming is shown in Figure 11. The oppositely directed suprathermal tails of the distribution during this interval are in marked contrast to the unidirectional heat flux signature normally observed.

As noted above, approximately half of all observed interplanetary bidirectional heat flux events have similar associations with interplanetary shocks. Delay times from shock passage to the onset of electron bidirectionality in these events is variable, but a typical delay is ~13 hours, corresponding to an average spatial separation of ~0.15 AU. Bulk plasma flows within these shock-associated bidirectional events are almost always substantially faster than are the ambient solar wind flows ahead of the shocks. By way of

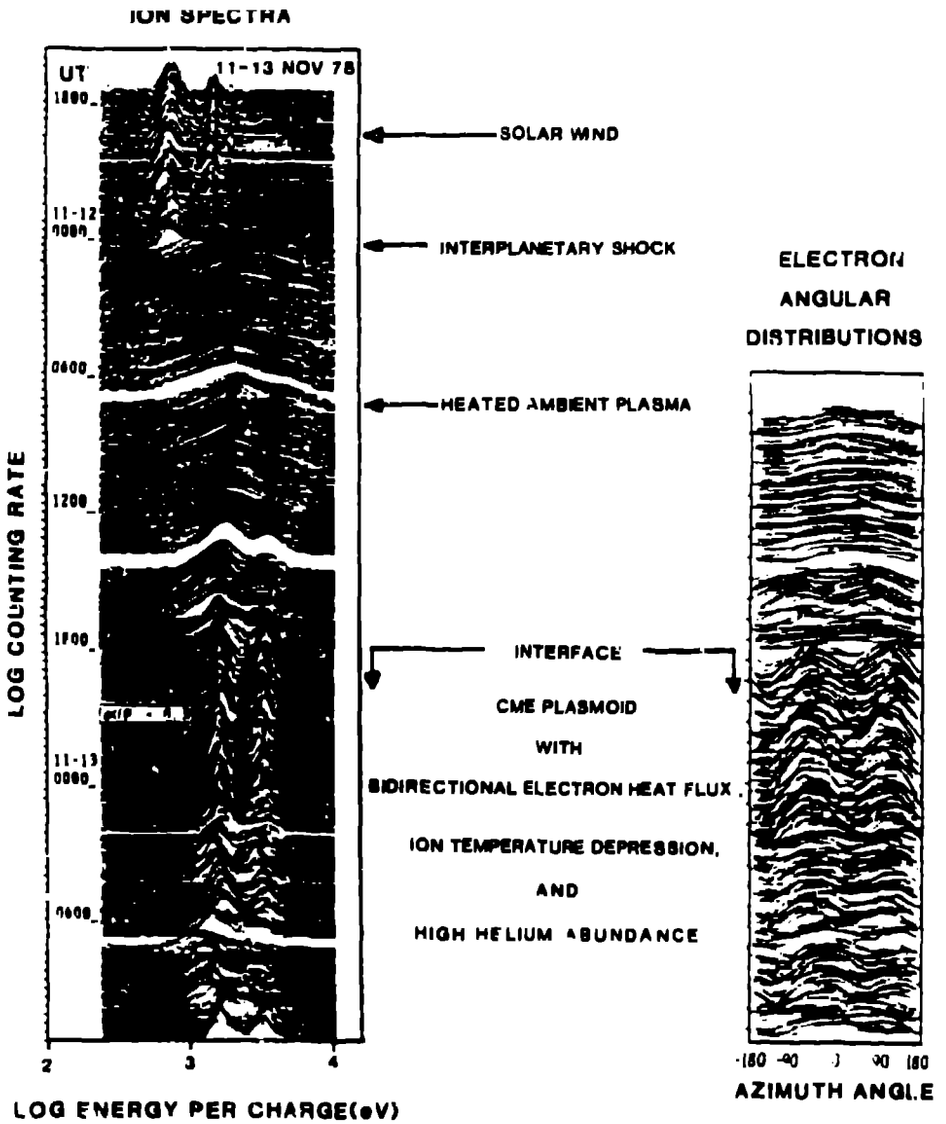

Fig. 10. On the left, a vertically stacked time series of one-dimensional solar wind ion E/q spectra obtained in the solar wind on November 11–13, 1978. Tic marks on the left denote factors of 10 differences in count rate. On the right, a time series of solar wind electron angular distributions integrated over energies greater than 100 eV. 0° viewing corresponds to detector viewing toward the sun. Tic marks on the left denote factors of 10 differences in count rate. Adapted from *Bame et al.* [1981].

contrast, for bidirectional events which are not shock-associated, bulk flow speeds are generally comparable to or slower than that of the ambient plasma ahead. Indeed, relative flow speed between the plasma within a bidirectional event and the ambient plasma ahead is the feature which best distinguishes events which are shock-associated from those which are not [*Gosling et al.*, 1987]. It is thus reasonable to suggest that (1) all (or at least most) interplanetary bidirectional events have similar solar origins, and (2) it is the relative speed between the bulk flows within such events and the ambient plasma ahead which determines whether or not a shock forms.

It has long been believed that most shock waves in the solar wind at 1 AU are a consequence of solar activity, e.g., solar flares, eruptive prominences, and that this activity must include the ejection of a significant mass (10^{15}–10^{16} gms) of material into the interplanetary medium [e.g., *Hundhausen*, 1972].

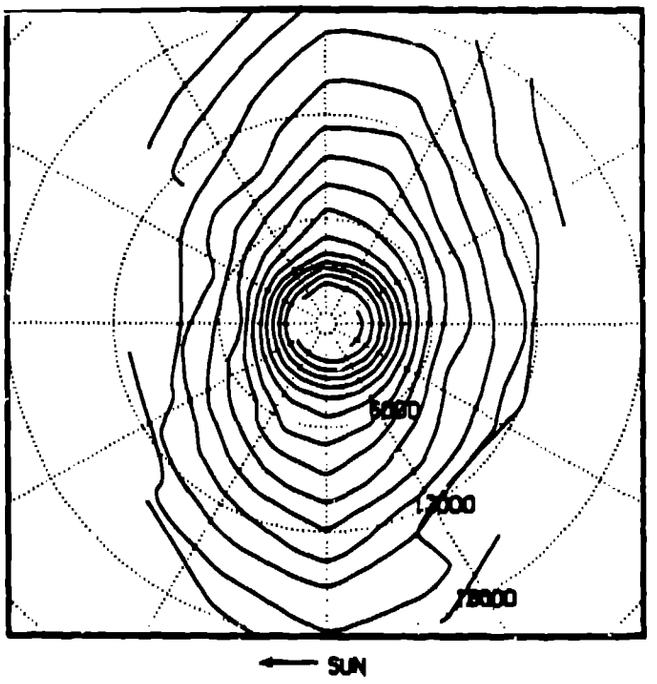

Fig. 11. Contours of a two-dimensional electron velocity distribution measured on November 12, 1978. Adjacent isointensity contours differ by a factor of 0.5 in log f, where f is phase space density.

Numerous studies relating interplanetary shocks observed at and inside of the Earth's orbit (1 AU) to observations of coronal mass ejections (CMEs) observed with orbiting coronagraphs (see, for example, the review by *Schwenn* [1986]) confirm this suggestion. Although CMEs with a wide range of speeds are observed [e.g., *Gosling et al.*, 1976; *Howard et al.*, 1985], only the fastest CMEs produce interplanetary shocks [e.g., *Sheeley et al.*, 1985].

Given the above associations, it should be clear that a bidirectional electron heat flux is one of the more prominent signatures of a CME in the solar wind at 1 AU. Figure 12 illustrates two possible ways the electron heat flux bidirectionality might arise in such events. It is generally believed that a CME represents the ejection of material into interplanetary space from regions in the corona that were not previously participating in the solar wind expansion. That is, the material there is on closed magnetic field lines which, owing to the high electrical conductivity of the plasma, are dragged outward from the sun with the ejecta. In the model illustrated in the upper portion of the figure these field lines disconnect from the sun to form an outward propagating plasmoid, while in the model illustrated in the bottom portion the field lines retain their connection to the sun and form a "magnetic bottle." In both models the bidirectional heat flux results initially because both ends of the magnetic loop are connected directly to the hot inner corona close to the sun. This, of course, is in contrast to the ambient solar wind expansion where field lines are "open," being connected at one end to the sun and at the other end to the outer heliosphere. In the reconnection (plasmoid) model the counterstreaming heat flux becomes trapped within the plasmoid as it disconnects from the sun. In either model a shock forms in front of the CME only if the ejection speed

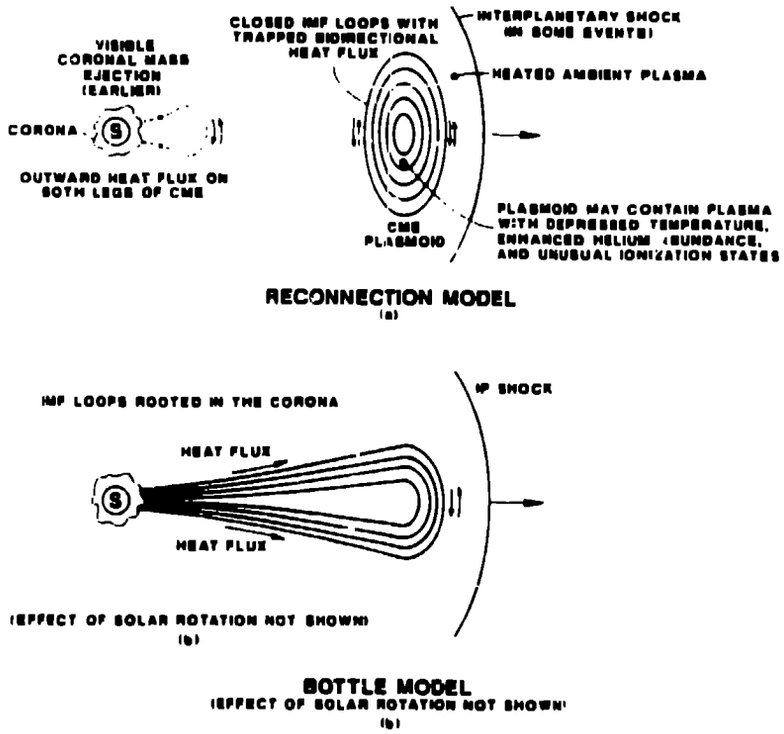

Fig. 12. Possible magnetic topologies associated with coronal mass ejections (CMEs) in the solar wind. In the upper example the CME has disconnected magnetically from the sun to form a closed, detached plasmoid. In the bottom example the CME retains its magnetic connection to the sun to form a magnetic bottle. In either case the bidirectional electron heat flux results initially because both ends of the field lines are connected to the hot inner corona. A shock forms in front of the CME only when the CME speed sufficiently exceeds the speed of the ambient plasma ahead.

sufficiently exceeds that of the ambient solar wind.

BIDIRECTIONAL ELECTRON HEAT FLUXES AND HEMISPHERICALLY SYMMETRIC POLAR RAIN

Although one normally thinks of the Earth as being shielded from direct contact with the solar wind by its extensive magnetosphere, there is considerable evidence that the solar wind electron heat flux commonly penetrates to very low altitudes in the Earth's polar cap regions. The evidence comes in the form of precipitating electrons with energies greater than about 100 eV which are present almost continuously at the top of the Earth's atmosphere in one or the other of the polar regions, but usually not both simultaneously. This precipitation is known as polar rain [*Winningham and Heikkila*, 1974], and it has long been recognized that the asymmetry between the precipitation in the different polar caps is strongly correlated with the polarity of the IMF [e.g., *Fennell et al.*, 1977; *Meng and Kroehl*, 1977]. When the IMF is directed outward from the sun along the nominal Archimedean spiral, polar rain occurs predominantly in the northern polar cap, and when it points inward toward the sun, polar rain occurs predominantly in the southern polar cap.

The connection between the solar wind electron heat flux and polar rain can be understood if (1) mag

field lines in the polar caps are "open" to interplanetary space and (2) as previously noted, the $\gtrsim 80$ eV electrons which carry the solar wind heat flux behave largely like test particles and thus travel relatively freely along these open field lines from the solar wind down to the polar caps. The "open" character of polar cap field lines is, of course, a consequence of the fact that field lines in the polar cap are magnetospheric field lines that originally become interconnected to the IMF at the dayside magnetopause and are subsequently dragged into the geomagnetic tail lobes by the flow of the solar wind past the Earth [e.g., *Crooker*, 1977].

Figure 13 illustrates the origin of the usual asymmetry of the polar rain precipitation in the different polar caps. Depending on the polarity of the IMF, usually only one of the polar caps is magnetically connected to the sun, the other polar cap being magnetically connected to the outer heliosphere. Thus, when the IMF is directed outward from the sun (upper panel) the electron heat flux streams into the northern polar cap, and when the IMF is directed in toward the sun (lower panel) the electron heat flux streams into the southern polar cap.

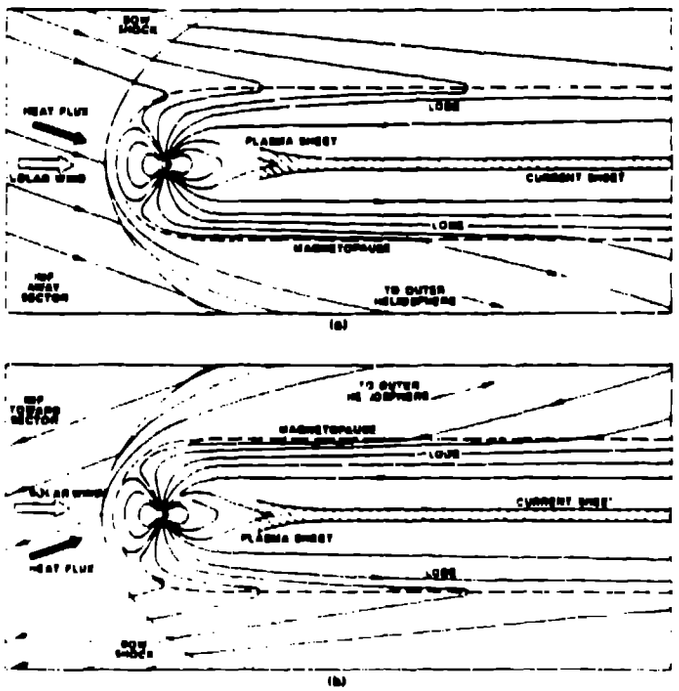

Fig. 13. Schematic drawings illustrating the interconnection of the terrestrial field with the IMF for an outward directed IMF (upper panel) and an inward directed IMF (lower panel). In the former case the solar wind electron heat flux is directed into the northern tail lobe and polar cap, and in the latter it is directed into the southern tail lobe and polar cap.

It is worth noting that only those heat flux electrons travelling nearly parallel to the field are able to penetrate to low altitudes to produce polar rain; the remainder of the electrons are mirrored by the increasingly stronger magnetic field at lower altitudes and return outward to interplanetary space. Thus, counterstreaming electron fluxes are commonly observed in one or the other of the tail lobes [*Fairfield* and *Scudder*, 1985; *Baker et al.*, 1986]. The bidirectional fluxes observed there should contain field-aligned

loss cones in the return (tailward) direction owing to the loss of particles which actually precipitate in the upper atmosphere. However, such loss cones should be quite narrow (1° 2°) and are difficult to detect with present instrumentation.

On occasion satellites in low Earth orbit have detected polar rain events where the flux of electrons is simultaneously nearly the same in both polar caps [*Makita* and *Meng*, 1987]. Such events are known as hemispherically symmetric polar rain to contrast them with the asymmetric precipitation which generally prevails. Hemispherically symmetric polar rain events have typical durations of ~10 hours, occur about once per month on the average, and often occur within 24 hours after the Earth passage of interplanetary shocks.

Figure 14 relates the timing of one such hemispherically symmetric polar rain event to interplanetary

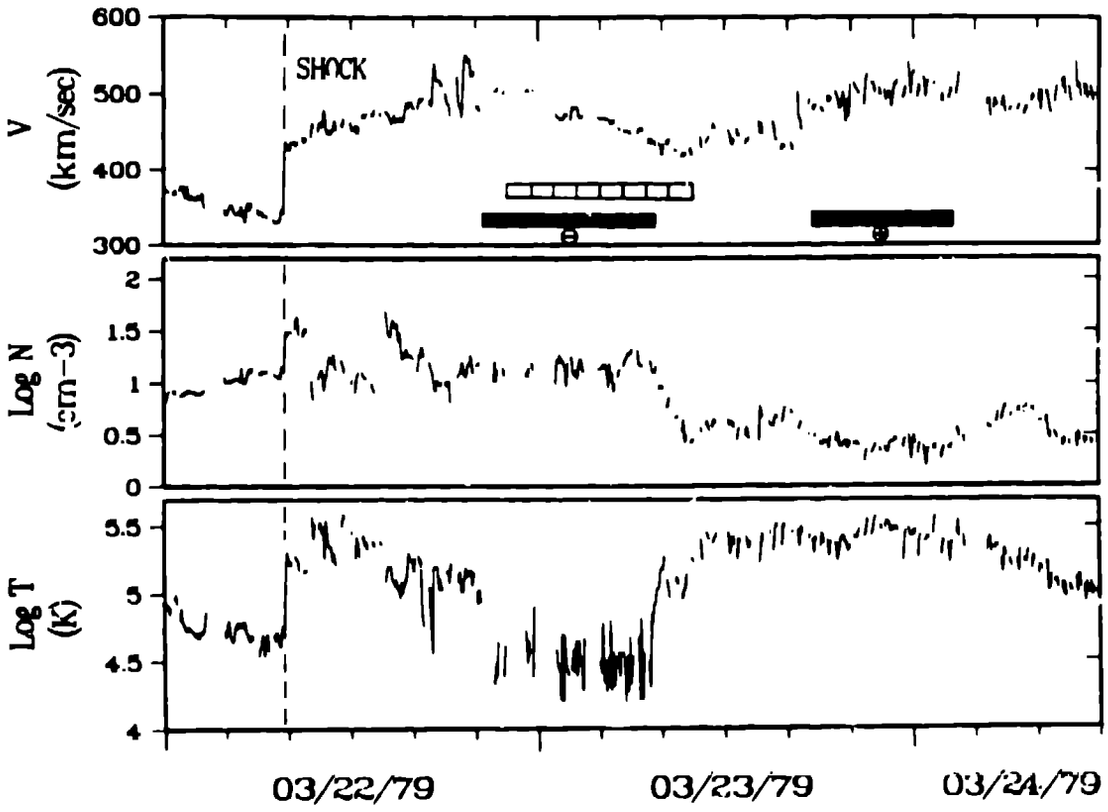

Fig. 14. Solar wind proton parameters measured in the March 22–24, 1979 interval. From top to bottom the quantities plotted are the bulk flow speed, the log of the density, and the log of the temperature. The solid horizontal bars beneath the speed profile indicate observed CMEs (bidirectional electron heat flux events) while the hatched bar beneath the speed profile denotes the time of a hemispherically symmetric polar rain event at Earth. The circled + and − beneath the solid horizontal bars denote the predominant sign of the out-of-the-ecliptic component of the IMF (that is, the sign of B_z) during the bidirectional events. From *Gosling et al.* [1986b].

conditions as measured by ISEE 3 236 R_E upstream from Earth [*Gosling et al.*, 1986b]. A strong interplanetary shock passed the spacecraft at 0748 UT on March 22, 1979, giving rise to the discontinuous jumps in proton bulk flow speed, density, and temperature observed at that time. A strong bidirectional electron heat flux event was detected following the shock beginning at 2030 UT on March 22 and persisting

until ~0710 UT on the following day. A second bidirectional event was encountered beginning at 1713 UT on March 23 and lasting until ~0215 UT on March 24. Both of these interplanetary events are indicated by the solid bars beneath the speed profile in the top panel of Figure 14. The first of these two events is undoubtedly the CME driving the shock.

An intense hemispherically symmetric polar rain event (nearly equal fluxes of precipitating electrons in both polar caps) began at ~ 2200 UT on March 22 and lasted until ~ 1000 UT the next day. This interval is indicated by the hatched bar beneath the speed profile in Figure 14. The relative timing between this polar cap event and the first of the interplanetary bidirectional events clearly indicates a causal association between the two phenomena, the lag between the interplanetary event and the polar cap event being related to the plasma travel time from the spacecraft to the Earth and to the finite time required for newly interconnected field lines to occupy a substantial fraction of the polar cap.

Despite the excellent correlation between the first interplanetary event and a hemispherically symmetric polar rain event, we note that the second interval of bidirectional streaming electrons apparently did not produce hemispherically symmetric polar rain. A major difference between the two interplanetary events was the sense of the tilt of the IMF relative to the ecliptic plane. In the first case the field was tipped primarily southward, while it pointed primarily northward during the second event. Thus the IMF orientation was favorable for dayside reconnection at the Earth's magnetopause (oppositely directed IMF and terrestrial field) in the first event, but was unfavorable during the second event. That is, interconnection between the Earth's field and the IMF is a necessary condition for the production of hemispherically symmetric polar rain when a bidirectional electron heat flux is present in interplanetary space.

Figure 15 illustrates the correspondence between all of the hemispherically symmetric polar rain events reported to date by *Makita and Meng* [1987] and interplanetary bidirectional heat flux events. Although the timing between these relatively rare phenomena is seldom as simple as in the March 22, 1979, events, there can be little question but that the bidirectional electron heat flux events are the source of hemispherically symmetric polar rain. This also demonstrates beyond doubt that the normal solar wind electron heat flux is the source of the more usual asymmetric polar rain.

Figure 16 provides a sketch, not to scale, of what we believe is the appropriate geometry of the Earth's field and the local IMF during the events we have been discussing. Hemispherically symmetric polar rain occurs when the local IMF has the form of either a closed loop, as drawn in the figure, or a magnetic bottle rooted at both ends in the sun (see bottom panel of Figure 12). Note that, in contrast to the usual situation where only one of the polar caps is magnetically connected to the sun (see Figure 13), we infer that during hemispherically symmetric polar rain events either both polar caps are connected to the sun or, as drawn in Figure 16, neither polar cap is connected to it.

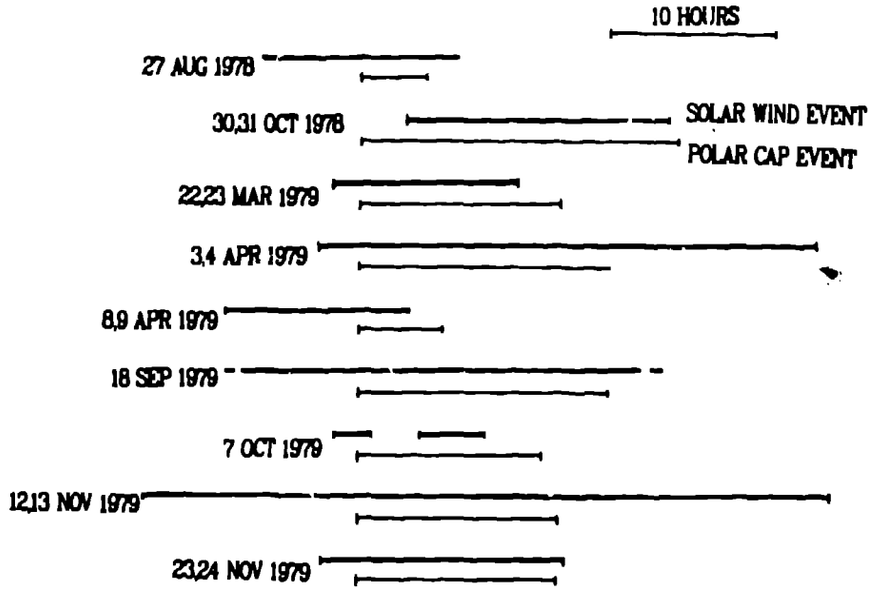

Fig. 15. Bar chart indicating the observed temporal relationship between all reported hemispherically symmetric polar rain events [*Makita* and *Meng*, 1987] and bidirectional electron heat flux events observed at ISEE 3 approximately 230 R_E upstream. For each example the interplanetary event is above and the polar cap event is below. The events are aligned vertically so that the onsets of all the polar cap events fall near the middle of the graph. Note that a bidirectional electron heat flux event was observed for all of the hemispherically symmetric polar rain events, and that for all events but one (30, 31 Oct. 1978) the interplanetary event started prior to the terrestrial event. The strong association demonstrated here between these two relatively rare and brief phenomena demonstrates that (1) the solar wind electron heat flux is the primary source of polar rain and (2) in particular, a bidirectional electron heat flux in the solar wind is responsible for hemispherically symmetric polar rain. Adapted from a table in *Gosling et al.* [1986b].

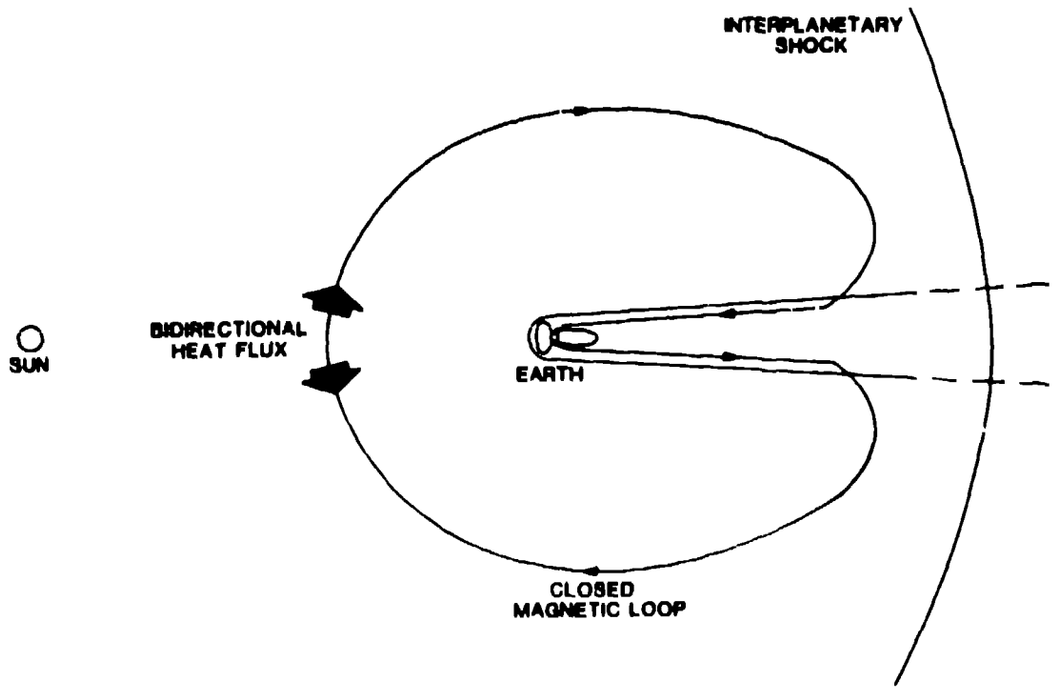

Fig. 16. Schematic illustration of the possible interconnection between the IMF and the terrestrial field during a hemispherically symmetric polar rain event. Although the interplanetary shock drawn is not an essential aspect of the interconnection, such shocks often form in front of the faster CMEs (bidirectional heat flux events). From *Gosling et al.* [1986b].

SUMMARY

The solar corona is much hotter than the vacuum of interplanetary space and, as a result, heat flows from the sun to the outer reaches of the heliosphere. In the solar wind the heat flux is transported primarily by the electrons, which are more mobile than the ions. Measurements reveal that this heat flux is carried primarily by electrons with energies above ~80 eV and is directed outward from the sun along the interplanetary magnetic field.

Occasionally a bidirectional electron heat flux is observed in interplanetary space. These bidirectional fluxes usually signal either magnetic connection to an additional hot source such as a planetary bow shock or cometary bow wave or spacecraft entry into a coronal mass ejection. In the former case the occurrence of bidirectionality can, among other things, be used to infer the overall shape of the bow shock or bow wave, while in the latter case the bidirectionality can be used to infer the closed magnetic topology of the CME.

Owing to the open nature of the magnetic field in the Earth's polar cap regions and the very high mobility of the electrons which carry the solar wind heat flux, a portion of the solar wind heat flux commonly penetrates to low altitudes to produce the precipitation known as polar rain. Intervals when polar rain is observed with nearly equal intensity in both polar caps correspond to times when the Earth is immersed within a CME at 1 AU and the solar wind electron heat flux is bidirectional. At such times both of the Earth's polar caps are either magnetically connected to the sun or are connected to a closed magnetic loop (plasmoid) which is entirely disconnected from the sun.

Acknowledgments. The results reviewed here were obtained in collaboration with a number of our colleagues, including D. N. Baker, W. C. Feldman, S. A. Fuselier, E. J. Smith, J. A. Stansberry, M. F. Thomsen, and R. D. Zwickl. This work was performed under the auspices of the U. S. Department of Energy with support from NASA under S-04039-D.

REFERENCES

Baker, D. N., S. J. Bame, W. C. Feldman, J. T. Gosling, R. D. Zwickl, J. A. Slavin, and E. J. Smith, Strong electron bidirectional anisotropies in the distant tail: ISEE 3 observations of polar rain, *J. Geophys. Res.*, **91**, 5637, 1986.

Bame, S. J., J. R. Asbridge, H. E. Felthauser, J. P. Glore, G. Paschmann, P. Hemmerich, K. Lehman, and H. Rosenbauer, ISEE 1 and 2 fast plasma experiment and the ISEE 1 solar wind experiment, *IEEE Trans. Geoscience Electronics*, **GE-16**, 216, 1978a.

Bame, S. J., J. R. Asbridge, H. E. Felthauser, J. P. Glore, H. L. Hawk, and J. C. Chavez, ISEE-C solar wind plasma experiment, *IEEE Trans. Geoscience Electronics*, **GE-16**, 160, 1978b.

Bame, S. J., J. R. Asbridge, W. C. Feldman, J. T. Gosling, and R. D. Zwickl, Bi-directional streaming of solar wind electrons >80 eV: ISEE evidence for a closed field structure within the driver gas of an interplanetary shock, *Geophys. Res. Lett.*, **8**, 173, 1981.

Bame, S. J., R. C. Anderson, J. R. Asbridge, D. N. Baker, W. C. Feldman, S. A. Fuselier, J. T. Gosling, D. J. McComas, M. F. Thomsen, D. T. Young, and R. D. Zwickl, Comet Giacobini-Zinner: Plasma description, *Science*, **232**, 356, 1986.

Crooker, N. U., The magnetospheric boundary layers: A geometrically explicit model, *J. Geophys. Res.*, **82**, 3629, 1977.

nd J. D. Scudder. Polar rain: Solar coronal electrons in the Earth's magnetosphere. *J.* **90**. 4055. 1985.
J. R. Asbridge. S. J. Bame. and M. D. Montgomery. Solar wind heat transport in the Earth's bow shock. *J. Geophys. Res.*. **78**. 3697. 1973.
J. R. Asbridge. S. J. Bame. M. D. Montgomery. and S. P. Gary. Solar wind electrons. *J.* **80**. 4181. 1975.
R. C. Anderson. J. R. Asbridge. S. J. Bame. J. T. Gosling. and R. D. Zwickl. Plasma re of magnetic connection to the Earth's bow shock: ISEE 3. *J. Geophys. Res.*. **87**. 632.

R. C. Anderson. S. J. Bame. S. P. Gary. J. T. Gosling. D. J. McComas. M. F. Thomsen. and M. M. Hoppe. Electron velocity distributions near the Earth's bow shock. *J. Geophys.* 83.
F. Mizera. and D. R. Croley. Low energy polar cap electrons during quiet times. *Conf. ic Ray Conf. 14th.* **4**. 1267. 1975.
. C. Feldman. S. J. Bame. E. J. Smith. and F. L. Scarf. Heat flux observations and the ransition region boundary of Giacobini-Zinner. *Geophys. Res. Lett.*. **13**. 247. 1986.
Hildner. R. M. MacQueen. R. H. Munro. A. I. Poland. and C. L. Ross. The speeds of ection events. *Solar Phys.*. **48**. 389. 1976.
Borrini. J. R. Asbridge. S. J. Bame. W. C. Feldman. and R. T. Hansen. Coronal streamers d at 1 AU. *J. Geophys. Res.*. **86**. 5438. 1981.
R. Asbridge. S. J. Bame. M. F. Thomsen. and R. D. Zwickl. Large amplitude. low ia fluctuations at Comet Giacobini-Zinner. *Geophys. Res. Lett.*. **13**. 267. 1986a.
N. Baker. S. J. Bame. and R. D. Zwickl. Bidirectional solar wind electron heat flux and symmetric polar rain. *J Geophys. Res.*. **91**. 11. 352. 1986b.
N. Baker. S. J. Bame. W. C. Feldman. R. D. Zwickl. and E. J. Smith. Bidirectional solar eat flux events. *J. Geophys. Res.*. **92**. 8519. 1987.
t. Sheeley. M. J. Koomen. and D. J. Michels. Coronal mass ejections: 1979-1981. *J.* **90**. 8173. 1985.
.. *Coronal Expansion and Solar Wind*. Springer-Verlag. New York. NY. 1972.
J.. An interplanetary view of coronal holes. in *Coronal Holes and High Speed Wind* by J. Zirker. p. 225. Colorado Associated University Press. Boulder. CO. 1977.
'.-I. Meng. Long-period polar rain variations. solar wind and hemispherically symmetric *eophys. Res.*. **92**. 7381. 1987.
J. T. Gosling. S. J. Bame. J. A. Slavin. E. J. Smith. and J. L. Steinberg. The Giacobini-tail: Tail configuration and current sheet. *J. Geophys. Res.*. **92**. 1139. 1987.
H. W. Kroehl. Intense uniform precipitation of low-energy electrons over the polar cap. .. **82**. 2305. 1977.
D.. S. J. Bame. and A. J. Hundhausen. Solar wind electrons: Vela 4 measurements. *J.* **73**. 4999. 1968.
D.. J. R. Asbridge. S. J. Bame. and W. C. Feldman. Solar wind electron temperature owing some interplanetary shock waves. Evidence for magnetic merging?. *J. Geophys.* 1974.
D. Scudder. and M Sugiura. Electron energy flux in the solar wind. *J. Geophys. Res.*.

. Schwenn. E. Marsch. B. Meyer. H. Miggenrieder. M. D. Montgomery. K. H. Muhlhauser. Voger. and S. M. Zink. A survey on initial results of the Helios plasma experiment. *J.* 31. 1977.
tionship of coronal transients to interplanetary shocks: 3D aspects. *Space Sci. Rev.*. **44**.

A. Howard. M. J. Koomen. D. J. Michels. R. Schwenn. K. H. Muhlhauser. and H. Rosen-mass ejections and interplanetary shocks. *J. Geophys. Res.*. **90**. 163. 1985.
'. Tsurutani. J. A. Slavin. D. E. Jones. G. L. Siscoe. and D. A. Mendis. ICE encounter Zinner: Magnetic field observations. *Science*. **232**. 382. 1986.
J. T. Gosling. M. F. Thomsen. S. J. Bame. and E. J. Smith. Interplanetary magnetic s associated with bidirectional electron heat fluxes detected at ISEE 3. submitted to *J.* 987.
S. J. Bame. W. C. Feldman. J. T. Gosling. D. J. McComas. and D. T. Young. The d transition region at Giacobini-Zinner. *Geophys. Res. Lett.*. **13**. 393. 1986.
and E. J. Smith. Strong hydromagnetic turbulence associated with Comet Giacobini-. *Res. Lett.*. **13**. 259. 1986.
.. and W. J. Heikkila. Polar cap auroral electron fluxes observed with ISIS 1. *J. Geophys.* 974.

of driver gas following interplanetary shocks observed by ISEE 3. *Solar Wind 5*. NASA Conf. Proceed., CP-2280. 711-717. 1983.

Zwickl, R. D., D. N. Baker, S. J. Bame, W. C. Feldman, S. A. Fuselier, W. F. Huebner, D. J. McComas, and D. T. Young, Three component plasma electron distribution in the intermediate ionized coma of Comet Giacobini-Zinner, *Geophys. Res. Lett.* **13**, 401, 1986.